J. Fluid Mech. (2023), *vol*. 958, A18, doi:10.1017/jfm.2023.109

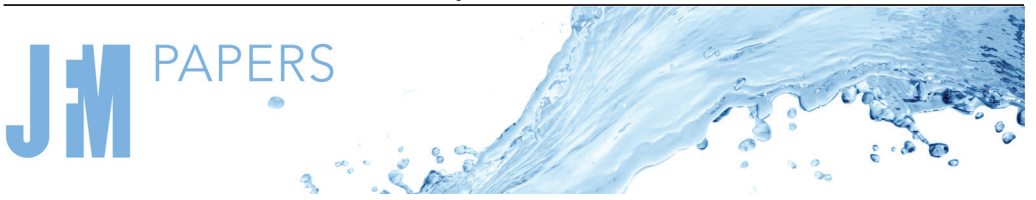

Droplet evaporation in inert gases

Huayong Zhao[1],† **and François Nadal**[1]

[1]Wolfson School of Mechanical, Electrical and Manufacturing Engineering, Loughborough University, Leicestershire LE11 3TU, UK

(Received 18 July 2022; revised 10 January 2023; accepted 29 January 2023)

A general mixed kinetic-diffusion boundary condition is formulated to account for the out-of-equilibrium kinetics in the Knudsen layer. The mixed boundary condition is used to investigate the problem of quasi-steady evaporation of a droplet in an infinite domain containing inert gases. The widely adopted local thermodynamic equilibrium assumption is found to be the limiting case of infinitely large kinetic Péclet number Pe_k, and it introduces significant error for $Pe_k \leqslant O(10)$, which corresponds to a typical droplet radius a of a few micrometres or smaller. When compared with experimental data, solutions based on the mixed boundary condition, which take into account the temperature jump across the Knudsen layer, better predict the time evolution of a than the classical D^2-law (i.e. $a^2 \propto t$, where t denotes time). In the slow evaporation limit, an analytical solution is obtained by linearising the full formulation about the equilibrium condition, which shows that the D^2-law can be recovered only in the large Pe_k limit. For small Pe_k, where the process is dominated by kinetics, a linear relation, i.e. $a \propto t$, emerges. When the gas phase density approaches the liquid density (e.g. at high-pressure or low-temperature conditions), the increase in the chemical potential of the liquid phase due to the presence of inert gases needs to be accounted for when formulating the mixed boundary condition, an effect largely ignored in the literature so far.

Key words: drops, condensation/evaporation

1. Introduction

Evaporation of droplets in inert gases occurs in a wide range of practical applications and have been investigated extensively since the pioneering work of Maxwell (1890). His approach of modelling the evaporation process based on macroscopic conservation laws assuming continuum liquid and gas phases has been proved adequate for sufficiently

† Email address for correspondence: h.zhao2@lboro.ac.uk

© The Author(s), 2023. Published by Cambridge University Press. This is an Open Access article, distributed under the terms of the Creative Commons Attribution licence (http://creativecommons.org/licenses/by/4.0/), which permits unrestricted re-use, distribution and reproduction, provided the original article is properly cited.

https://doi.org/10.1017/jfm.2023.109 Published online by Cambridge University Press

large droplets (i.e. Knudsen number $Kn = \lambda/a \ll 1$, where λ is the mean free path in the gas phase, and a is the droplet diameter) and is now widely adopted. Over the years, continued efforts have been made to correct for some of the assumptions made by Maxwell, such as the quasi-steady (QS) gas phase, negligible internal and external flow (including the Stefan flow) and negligible droplet heating, as reviewed in detail in the literature (Sazhin 2006; Sirignano 2010). However, the paradoxical assumption of the local thermodynamic equilibrium at the interface (net evaporation can occur only when the interface region is out of equilibrium) persists and is still widely adopted in recent theoretical and experimental work (Lu *et al.* 2017; Finneran, Garner & Nadal 2021). The local thermodynamic equilibrium assumption allows for the determination of the vapour partial pressure in the close vicinity of the droplet surface (hence the vapour concentration), based on the liquid surface temperature. As a result, it serves as a sufficient boundary condition to couple the transport process in the liquid phase to those in the gas phase through a continuum hydrodynamic model without considering the non-equilibrium kinetics. This approach is adopted widely in the modelling the evaporation of isolated droplets (Sazhin 2006; Sirignano 2010; Holyst *et al.* 2013*a*) and also droplets on an impermeable substrate (Deegan *et al.* 1997, 2000; Poulard, Be & Cazabat 2003).

Meanwhile, in experimental and theoretical work dealing with evaporation of droplets in their own vapour (Lu *et al.* 2019; Rana, Lockerby & Sprittles 2019), the local thermodynamic equilibrium is replaced by a more rigorous out-of-equilibrium kinetic boundary condition where the evaporative mass flux J depends on the difference in the chemical potential between the liquid and the vapour phase. This kinetic boundary condition enables the decoupling of the low Mach number gas phase from the liquid phase, so a 'one-sided' model can be developed to model the liquid evaporation dynamics. Due to this convenience, the one-sided model was also used frequently in modelling the dynamics of an evaporating liquid film (Burelbach, Bankoff & Davis 1988; Oron, Davis & Bankoff 1997; Craster & Matar 2009). Assuming the evaporative mass flux across the out-of-equilibrium kinetic region – i.e. the Knudsen layer – should equal the mass flux out of this region, a mixed kinetic-diffusion boundary condition can be formulated to couple the liquid and gas phases (Kryukov, Levashov & Sazhin 2004; Sultan, Boudaoud & Ben Amar 2005; Holyst *et al.* 2013*a*). Sultan *et al.* (2005) also identified the kinetic Péclet number $Pe_k = u_k H/\mathcal{D}_{AB}$ (where u_k is the typical kinetic velocity, H is the characteristic length and $\mathcal{D}_{AB}$ is the mass diffusivity between the liquid A and the inert gas B) to be the key dimensionless group, and showed that the local thermodynamic equilibrium assumption corresponds to the limiting case of an infinitely large Pe_k. When formulating the boundary condition, existing works focused on slow evaporation (thus ignoring the Stefan flow) and adopted the widely used Hertz–Knudsen (HK) relation (Knudsen 1950) – i.e. (1.1) – to model the kinetics of net evaporation

$$J = \frac{1}{\sqrt{2\pi R_s^A}}\left(\sigma_e \frac{p_s^A}{\sqrt{T_s}} - \sigma_c \frac{p_k^A}{\sqrt{T_k}}\right). \tag{1.1}$$

In this expression, σ_e and σ_c are empirical evaporation and condensation coefficients, (p_s^A, T_s) and (p_k^A, T_k) are the vapour pressure of species A and temperature on the liquid surface and just outside the Knudsen layer, respectively, and R_s^A is the specific gas constant of species A. The HK relation was originally derived based on the assumption of an equilibrium Maxwellian velocity distribution in the gas phase and decoupled evaporation and condensation processes (i.e. σ_e and σ_c are constants). The HK relation is considered as semi-empirical, due to the absence of explicit expressions for σ_e and σ_c. Analytical expressions for σ_e and σ_c based on the statistical rate theory in the

https://doi.org/10.1017/jfm.2023.109 Published online by Cambridge University Press

thermal-energy-dominated limit (TED-SRT) were recently proposed by Persad & Ward (2016), as shown in (1.2*a*,*b*) and (1.3*a*–*c*)

$$\sigma_e = \frac{p_s^A}{p_k^A}\widehat{\sigma_e}, \quad \sigma_c = \sqrt{\overline{T_K}}\exp\left[-(N+4)(1-\overline{T_K})\right]\overline{T_K}^{-(N+4)}, \tag{1.2a,b}$$

where

$$\widehat{\sigma_e} = \exp\left[(N+4)(1-\overline{T_K})\right]\overline{T_K}^{N+4}, \quad \overline{T_K} = \frac{T_k}{T_s} = 1+\overline{\delta T}, \quad \overline{\delta T} = \frac{T_k - T_s}{T_s}. \tag{1.3a–c}$$

In these expressions, N is the number of internal vibration degrees of freedom (which is $3n-6$ for nonlinear molecules consisting of n atoms and $3n-5$ for linear molecules). Experimental data reviewed by Persad & Ward (2016) suggest that $\overline{\delta T}$ is typically much smaller than unity, so that $\hat{\sigma}_e$ and σ_c can be linearised about $\overline{T_k}=1$, which yields $\hat{\sigma}_e = 1+O(\overline{\delta T}^2)$ and $\sigma_c = 1+\overline{\delta T}/2+O(\overline{\delta T}^2)$. The TED-SRT formulation shows that both σ_e and σ_c are explicit functions of p_s, T_s, p_k and T_k, so that the evaporation and condensation processes are coupled. As highlighted by Persad & Ward (2016), considering T_k is always larger than T_s in cases of net evaporation, it is clear that $\sigma_c > 1$ during the evaporation. Therefore, the conventional interpretation that σ_c represents the fraction of molecules condensed into liquid on reaching the liquid surface is not physically sound. Sultan *et al.* (2005) set $\sigma_e = \sigma_c = 1$ and $T_s = T_k$ (a common approach adopted in the literature) which *de facto* implies thermodynamic equilibrium in the Knudsen layer (Persad & Ward 2016). In addition, in (1.1), p_s is commonly taken to be the saturated pressure $p_s^\star$ of the pure substance without correcting for its change due to the presence of inert gases. The impact of adopting this mixed boundary condition and relevant simplifications on predicting the evaporation rate of a droplet has yet to be quantified.

In this work, we derive more general mixed kinetic-diffusion boundary conditions that take into account the Stefan flow (§ 2). The mixed boundary condition is formulated based on either the semi-empirical HK model or the analytical TED-SRT model and includes corrections for the change of liquid chemical potential due to the presence of inert gas and the temperature jump across the Knudsen layer. The mixed boundary condition is then applied to investigate the problem of QS evaporation of a spherical droplet in an infinite domain containing inert gases. The full and linearised solutions for the QS evaporation problem are presented in § 3. The analytical and numerical results are then compared with the experimental data reported in the literature. The comparison shows the potential errors caused by the local thermodynamic equilibrium assumption and the neglect of the change of the chemical potential of the liquid phase (i.e. the effect of the inert gas). Conclusions regarding the impact of such a generalised mixed kinetic-diffusion boundary condition on the evaporation rate, and future work, are presented in the final section.

2. Formulation of the mixed boundary conditions

We consider here a spherical droplet of size a of pure substance A evaporating in an infinite gas domain that consists of vapour A and inert immiscible gases B, as in figure 1. When required, partial properties of a pure substances (e.g. evaporating substance A or inert gas B) are denoted using superscripts A and B, respectively, whereas properties of the whole gas phase (i.e. the mixture of gaseous A and the inert gas B) have no superscript. Throughout the article, the superscript l stands for the liquid domain. All quantities evaluated at the liquid interface and just outside the Knudsen layer are labelled with subscripts s and k, respectively.

https://doi.org/10.1017/jfm.2023.109 Published online by Cambridge University Press

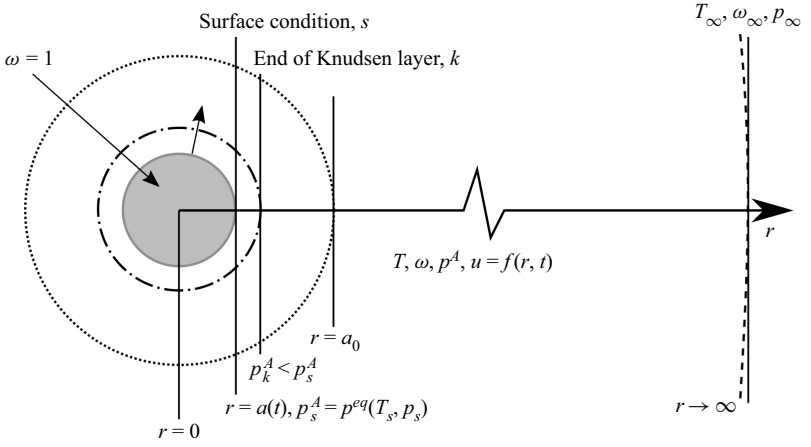

Figure 1. Illustration of the evaporation of a droplet in an infinite gas domain. Note that the Knudsen layer represents the conceptual out-of-equilibrium kinetic region: its outer boundary is not sharp due to the continuity of the partial pressure and temperature.

2.1. *Mass conservation across the Knudsen layer*

Assuming an infinitely thin Knudsen layer, mass conservation requires that

$$J = \rho_k(\boldsymbol{u}_k - \boldsymbol{u}_s) \cdot \hat{\boldsymbol{n}}, \tag{2.1}$$

where ρ is the density, $\boldsymbol{u}$ is the velocity and $\hat{\boldsymbol{n}}$ is the normal outward unit vector. The immiscibility of B in A results in a vanishing mass flux of B across the interface, such that the evaporation mass flux equals the mass diffusion flux of A, which can be written as

$$J = J_k^A = -\frac{\rho_k \mathcal{D}_{AB}[\nabla\omega \cdot \hat{\boldsymbol{n}}]_k}{1-\omega_k} = \frac{\rho_k \mathcal{D}_{AB}[\nabla\Phi \cdot \hat{\boldsymbol{n}}]_k}{\Phi_k}, \tag{2.2}$$

where ω is the mass fraction of A, and $\Phi = 1 - \omega$. Here, we consider the case where the total pressure in the gas domain remains unchanged (i.e. $Ma \ll 1$). In the case of high Mach number, the pressure relaxation process in the gas domain needs to be accounted for to find the change in pressure. To proceed, a kinetic model within the Knudsen layer (e.g. the analytical TED-SRT model or the semi-empirical HK model) needs to be used to predict J.

2.2. *The HK-based mixed boundary condition*

Assuming that the Knudsen layer is not too far from thermodynamic equilibrium and the velocity profile in the gas domain is Maxwellian, Struchtrup *et al.* (2017) proposed the following kinetic model in a pure vapour environment, based on the extension of the Onsager–Casimir reciprocity relations:

$$\begin{bmatrix} \dfrac{p_s^{eq} - p_k}{\sqrt{2\pi R_s^A T_s}} \\ -\dfrac{p_s^{eq}}{\sqrt{2\pi R_s^A T_s}} \dfrac{T_s - T_k}{T_s} \end{bmatrix} = \begin{bmatrix} r_{11} & r_{12} \\ r_{21} & r_{22} \end{bmatrix} \begin{bmatrix} J \\ \dfrac{q_v}{R_s^A T_s} \end{bmatrix}, \tag{2.3}$$

where coefficients $r_{11} = 1/\pi + 9/32$, $r_{12} = r_{21} = 1/16 + 1/(5\pi)$, $r_{22} = 1/8 + 13/(25\pi)$, p_s^{eq} is the equilibrium vapour pressure of species A and q_v is the heat flux adds to

https://doi.org/10.1017/jfm.2023.109 Published online by Cambridge University Press

the vapour. In the case of a negligible change of sensible heat inside the droplet, $q_v = -J\mathcal{L}$, where $\mathcal{L}$ is the latent heat of evaporation. The above expression is an extension of the HK model taking into account the Stefan flow due to net evaporation, with the additional assumption $\sigma_e = \sigma_c = 1$. It also predicts the temperature jump across the Knudsen layer, which is commonly ignored in the literature. As shown by Persad & Ward (2016), assuming either $T_k = T_s$ or $\sigma_e = \sigma_c$ does not introduce major discrepancies compared with experimental results ($\leqslant 5\,\%$), but making both assumptions simultaneously forces the Knudsen layer into equilibrium, which could lead to significant errors. When applied in an inert gas environment, while the form of (2.3) might hold as long as the Knudsen layer is not too far from equilibrium, i.e. a linear irreversible process, the coefficients and p_s^{eq} should be corrected by taking into account inert gases. The effect of inert gases on the temperature jump is evidenced by the empirical correlation (2.4) proposed by Holyst *et al.* (2013*b*). Equation (2.4) is based on curve fitting of data obtained from molecular dynamic (MD) simulations of the evaporation of a droplet made of a Lennard–Jones fluid in inert gases and reads as

$$\frac{T_k - T_s}{T_\infty - T_s} = \frac{1}{1 + a/(C\lambda)}, \tag{2.4}$$

where C is a fitting parameter calculated to be 2.35, and λ is the mean free path of inert gas molecules. Equation (2.4) shows that a smaller λ leads to a smaller temperature jump. This makes sense because the thermalisation process becomes more efficient as the collision frequency increases at reduced λ.

When the liquid surface is assumed to be at thermodynamic equilibrium, p_s^{eq} can be determined by equating the chemical potential of the liquid phase μ^l and that of the vapour phase μ^v. In order to find the change of chemical potential due to the presence of inert gases, we consider an isothermal gas addition process. The chemical potentials of the liquid phase and vapour phase of A in the absence of any inert gas at temperature T_s and pressure $p_s^\star$ are denoted by $\mu^{l\star}$ and $\mu^{v\star}$. As the inert gas is added to the system to reach a new equilibrium at increased total pressure p_s, one obtains

$$\mu^l(T_s, p_s) - \mu^{l\star}(T_s, p_s^\star) = \mu^v(T_s, p_s^{eq}) - \mu^{v\star}(T_s, p_s^\star). \tag{2.5}$$

Applying the Gibbs–Duhem equation yields

$$\int_{p_s^\star}^{p_s} v^l \,\mathrm{d}p = \int_{p_s^\star}^{p_s^{eq}} v^v \,\mathrm{d}p, \tag{2.6}$$

where v^l, v^v and $v^{v\star}$ are molar volume of A in liquid phase, and the vapour phase with and without inert gas, respectively. In the case of constant liquid molar volume and ideal gases, one obtains

$$p_s^{eq} = p_s^\star(T_s)\exp(\overline{v_s}), \quad \text{with } \overline{v_s} = v^l\left(\frac{1}{v^v} - \frac{1}{v^{v\star}}\right). \tag{2.7}$$

It appears from (2.7) that the exponential correction factor could become significant as the specific volume ratio increases, e.g. at high system pressure or low gas temperature. Note that the assumption of ideal gas needs to be corrected at high pressure or very low temperature. To assess the value of $p_s^\star$, the Clausius–Claperon equation – which is derived assuming (i) an ideal gas law, (ii) negligibly small gas phase density (compared with that of the liquid phase) and (iii) constant latent heat – can be integrated between the local

https://doi.org/10.1017/jfm.2023.109 Published online by Cambridge University Press

equilibrium conditions at far field (i.e. outside the boundary layer) and that at the liquid surface. One obtains

$$p_s^\star = p_\infty \exp\left[\frac{\mathcal{L}}{R_s^A}\left(\frac{1}{T_\infty^{sat}} - \frac{1}{T_s}\right)\right], \tag{2.8}$$

where all properties at infinity are labelled with the subscript ∞. In the previous expression, T_∞^{sat} is the saturated temperature at p_∞.

By combining (2.2), (2.3), (2.7) and (2.8), and accounting for the surface tension σ_T based on Kelvin's law, we obtain the following mixed kinetic-diffusion boundary condition based on HK model:

$$\sqrt{\frac{1}{2\pi R_s^A T_s}}\left\{c_1 p_\infty \exp\left[\frac{\mathcal{L}}{R_s^A}\left(\frac{1}{T_\infty^{sat}} - \frac{1}{T_s}\right) + \overline{v_s} + \frac{\bar{\sigma}}{a}\right] - \left(c_1 + c_2\overline{\Delta T}\right) p_k^A\right\} = \frac{\rho_k \mathcal{D}_{AB}[\nabla \Phi \cdot \hat{\boldsymbol{n}}]_k}{\Phi_k}, \tag{2.9}$$

where $c_1 = r_{22}/(r_{11}r_{22} - r_{12}^2)$, $c_2 = c_1 r_{11}/r_{22}$ and $\bar{\sigma} = 2\sigma_T/(R_s^A T^l \rho^l)$.

2.3. *The TED-SRT-based mixed boundary condition*

Combining the analytical TED-SRT formulation derived by Persad & Ward (2016), i.e. (1.2*a*,*b*), together with (2.2), (2.7) and (2.8), and accounting for the surface tension, the following mixed boundary conditions can be derived:

$$\sqrt{\frac{1}{2\pi R_s^A}}\left\{\hat{\sigma}_e \frac{\left\{p_\infty \exp\left[\frac{\mathcal{L}}{R_s^A}\left(\frac{1}{T_\infty^{sat}} - \frac{1}{T_s}\right) + \overline{v_s} + \frac{\bar{\sigma}}{a}\right]\right\}^2}{p_k^A \sqrt{T_s}} - \sigma_c \frac{p_k^A}{\sqrt{T_k}}\right\} = \frac{\rho_k \mathcal{D}_{AB}[\nabla \Phi \cdot \hat{\boldsymbol{n}}]_k}{\Phi_k}. \tag{2.10}$$

2.4. *Dimensionless forms of the mixed boundary conditions*

To make the mixed kinetic-diffusion boundary conditions (2.9) and (2.10) dimensionless, the initial droplet radius a_0, the initial Stefan flow gas velocity $\mathcal{D}_{AB}/a_0$ and the quantity $a_0^2/\mathcal{D}_{AB}$ are chosen as the typical length, velocity and time, respectively. The quantity ρ_∞ is chosen as the typical gas density, such that the typical evaporative mass flux becomes $\rho_\infty \mathcal{D}_{AB}/a_0$.

The mixed boundary condition based on the TED-SRT model (2.10) can be written in a dimensionless form as

$$\frac{\ln(B_M + 1)}{Pe_k} = \frac{\bar{p}^2 \exp(2\chi)\hat{\sigma}_e \sqrt{1 + \overline{\delta T}}\left[\varepsilon(\Psi + 1 - \Phi_\infty)^{-1} - (\varepsilon - 1)\right]^2 - \sigma_c}{(1 - \Phi_\infty + \varepsilon\Phi_\infty)^{-1}(1 - \kappa)^{1/2}[\varepsilon(\Psi + 1 - \Phi_\infty)^{-1} - (\varepsilon - 1)]}, \tag{2.11}$$

https://doi.org/10.1017/jfm.2023.109 Published online by Cambridge University Press

where

$$B_M = \frac{\omega_{QS,k} - \omega_\infty}{1 - \omega_{QS,k}}, \quad B_T = \frac{c_p^A}{\mathcal{L}}(T_\infty - T_{QS,k}), \tag{2.12a}$$

$$Pe_k = \frac{u_k a}{\mathcal{D}_{AB}}, \quad u_k = \left(\frac{R_s^A T_\infty}{2\pi}\right)^{1/2}, \quad \bar{p} = \frac{p^\star(T_\infty)}{p_\infty}, \quad \varepsilon = \frac{M^A}{M^B}, \tag{2.12b}$$

$$\Psi = \frac{\Phi_\infty B_M}{B_M + 1}, \quad \chi = \frac{\gamma}{\gamma - 1}\left(\frac{1}{Ja} - \frac{1 + \overline{\delta T}}{Ja - B_T}\right) + \overline{v_s} + \frac{\bar{\sigma}}{a}, \tag{2.12c}$$

$$Ja = \frac{c_{p,\infty}^A T_\infty}{\mathcal{L}}, \quad \kappa = \frac{B_T}{Ja}, \quad \overline{v_s} = \bar{\rho}[1 + (\varepsilon - 1)\Phi_\infty](1 - \bar{p}), \quad \bar{\rho} = \frac{\rho_\infty}{\rho^l}. \tag{2.12d}$$

In the above expressions, γ is the specific heat capacity ratio, c_p is the specific heat capacity, Ja is the Jakob number, B_M and B_T are the Spalding heat and mass transfer numbers, respectively, and $T_{QS,k}$ and $\omega_{QS,k}$ are the temperature and mass fraction obtained from the QS solutions.

The mixed boundary condition based on the HK formulation (2.9) can also be made dimensionless in the same way, which yields

$$\frac{\ln(B_M + 1)}{Pe_k} = \frac{\sqrt{1 + \overline{\delta T}}\{c_1[B_M + 1 + (\varepsilon - 1)\Phi_\infty]\bar{p}\exp(\chi) - (B_M + 1 - \Phi_\infty)(c_1 + c_2\overline{\delta T})\}}{\sqrt{1 - \kappa}\,[\varepsilon(B_M + 1) - (\varepsilon - 1)(B_M + 1 - \Phi_\infty)]\,(1 - \Phi_\infty + \varepsilon\Phi_\infty)^{-1}}. \tag{2.13}$$

Similarly, the analytical temperature jump model developed for evaporation in the pure vapour environment, i.e. (2.3) can be non-dimensionalised to become

$$\overline{\delta T} = \frac{\ln(B_M + 1)}{Pe_k}\left[r_{12} - r_{22}\frac{\gamma(\overline{\delta T} + 1)}{(\gamma - 1)(Ja - B_T)}\right]\frac{\sqrt{1 - \kappa}}{\bar{p}\exp(\chi)[\varepsilon - (\varepsilon - 1)(1 - \Phi_\infty)]}. \tag{2.14}$$

The empirical temperature jump model proposed for the evaporation in inert gases, i.e. (2.4), can be recast dimensionlessly as

$$\overline{\delta T} = \frac{\kappa}{(1 - \kappa)(1 + \tilde{a}\bar{\lambda}) - 1}, \quad \text{with } \bar{\lambda} = \frac{a_0}{C\lambda}. \tag{2.15}$$

Both (2.11) and (2.13) show that the validity of the assumption of local thermodynamic equilibrium depends on the value of Pe_k. As $Pe_k \to \infty$, the infinitely fast kinetic convection process instantaneously smooths out any imbalance in the chemical potential difference across the Knudsen layer – i.e. left-hand sides of (2.11) and (2.13) $\to 0$ – so the Knudsen layer will instantaneously be in thermodynamic equilibrium. The evaporation rate is then limited by the mass diffusion of A out from the Knudsen layer. One can also see from (2.14) that $\overline{\delta T} \to 0$ as $Pe_k \to \infty$. When $Pe_k \to \infty$, both (2.11) and (2.13) can be significantly simplified, and one obtains

$$B_T = Ja - \left\{\frac{1}{Ja} + \frac{\gamma - 1}{\gamma}\left[\ln\left(\frac{B_M + 1 + (\varepsilon - 1)\Phi_\infty}{B_M + 1 - \Phi_\infty}\right) + \ln(\bar{p}) + \overline{v_s} + \frac{\bar{\sigma}}{a_0\tilde{a}}\right]\right\}^{-1}. \tag{2.16}$$

https://doi.org/10.1017/jfm.2023.109 Published online by Cambridge University Press

In the case where $\bar{p} \to 1$, and $\{\overline{v_s}, \bar{\sigma}\} \to 0$, (2.16) can be further simplified to recover the diffusion-dominated boundary condition (Finneran *et al.* 2021):

$$B_T = Ja - \left\{ \frac{1}{Ja} + \frac{\gamma - 1}{\gamma} \left[\ln \left(\frac{B_M + 1 + (\varepsilon - 1)\Phi_\infty}{B_M + 1 - \Phi_\infty} \right) \right] \right\}^{-1}. \tag{2.17}$$

3. Quasi-steady droplet evaporation

3.1. *Solution to the QS problem*

In cases where buoyancy is negligible (i.e. large Froude number) and the internal flow in the droplet is absent, the problem becomes spherically symmetric. With further assumptions of a QS incompressible ideal gas phase, negligible pressure work and viscous dissipation (i.e. small Eckert number), constant fluids properties and in the absence of the Soret/Dufour effect and droplet heating, we obtain the following classical formulation of the problem (Spalding 1979; Abramzon & Sirignano 1989; Finneran *et al.* 2021):

$$\frac{\mathrm{d}\tilde{a}^2}{\mathrm{d}\tilde{t}} = -2\bar{\rho}\frac{Le}{\overline{c_p}} \ln(1 + B_T), \tag{3.1}$$

$$B_M + 1 = (B_T + 1)^{Le/\overline{c_p}}, \tag{3.2}$$

where $\tilde{a}$ and $\tilde{t}$ are the rescaled droplet size and time, respectively, $Le = k_\infty/(c_{p,\infty}\rho_\infty \mathcal{D}_{AB})$ is the Lewis number, k is the thermal conductivity and $\overline{c_p} = c^A_{p,\infty}/c_{p,\infty}$.

Note that both (2.17) and (3.2) are independent of the droplet size $\tilde{a}$ so B_M and B_T are constants during evaporation under the local thermodynamic assumption (i.e. the limit of $Pe_k \to \infty$), which leads to the classical D^2-law, i.e. $\tilde{a}^2 \propto \tilde{t}$. However, the D^2-law is no longer valid as we move away from this limit or the surface tension becomes important because both B_M and B_T will be functions of $\tilde{a}$. As Pe_k reduces, the chemical potential difference across the Knudsen layer increases so the local thermodynamic equilibrium assumption becomes less accurate. As $Pe_k \to 0$, the mass diffusion of A out from the Knudsen layer becomes more efficient than the kinetic process so that the evaporation rate is limited by the slow kinetics. As a result, the out-of-equilibrium kinetics becomes more prominent towards the end of the evaporation process. For a dilute gas, $\mathcal{D}_{AB} \sim T^{3/2}$, $u_k \sim T^{1/2}$, so $Pe_k \sim T^{-1}$ and the local thermodynamic equilibrium can more easily break down at high temperature.

The full problem of QS droplet evaporation can be solved numerically based on (3.1) and (3.2), together with the mixed kinetic-diffusion boundary conditions (e.g. (2.11) or (2.13)) and a temperature jump model (e.g. (2.14) or (2.15), or assuming negligible temperature jump). In this work, the numerical results were obtained based on the fourth-order Runge–Kutta methods with variable timesteps to ensure accuracy.

At the slow evaporation limit, the QS droplet evaporation problem based on (3.1), (3.2), (2.13) and (2.14) can be linearised about the equilibrium condition – i.e. $\{\overline{\delta T}, B_M, B_T\} = 0$ – to get

$$\frac{\mathrm{d}\tilde{a}^2}{\mathrm{d}\tilde{t}} = -2\bar{\rho}B_M, \quad B_M = \frac{Le}{\overline{c_p}}B_T, \quad s_1^{IT}\overline{\delta T} + \frac{s_2^{IT}}{Pe_k}B_M = 0, \tag{3.3a–c}$$

$$\left[\frac{1}{Pe_k} + \frac{c_1\bar{p}\bar{\sigma}\,\Omega_\infty(\varepsilon - 1)}{a_0\tilde{a}} + s_1^{HK}\right] B_M + s_s^{HK}B_T + s_3^{HK}\overline{\delta T} = s_4^{HK}, \tag{3.4}$$

https://doi.org/10.1017/jfm.2023.109 Published online by Cambridge University Press

where

$$s_1^{HK} = c_1\left[\bar{p}(1+\overline{v_s})(\varepsilon-1)\Phi_\infty + \Phi_\infty\right], \quad s_2^{HK} = c_1\bar{p}\frac{\gamma[1+(\varepsilon-1)\Phi_\infty]}{(\gamma-1)(Ja)^2}, \tag{3.5a}$$

$$s_3^{HK} = c_1\bar{p}\frac{\gamma\,[1-(\varepsilon-1)\Phi_\infty]}{(\gamma-1)Ja} + c_2(1-\Phi_\infty), \tag{3.5b}$$

$$s_4^{HK} = c_1\left\{\bar{p}\,[1+(\varepsilon-1)\Phi_\infty] - 1 + \Phi_\infty\right\}, \tag{3.5c}$$

$$s_1^{IT} = \bar{p}[\varepsilon-(\varepsilon-1)(1-\Phi_\infty)], \quad s_2^{IT} = r_{12} - r_{22}\frac{\gamma}{(\gamma-1)Ja}. \tag{3.5d}$$

If (2.15) is used to predict the temperature jump,

$$s_1^{IT} = 1, \quad s_2^{IT} = -\frac{\overline{c_p}}{Le}\frac{Pe_k}{\tilde{a}\,Ja\,\bar{\lambda}}. \tag{3.6a,b}$$

The rescaled TED-SRT relation, i.e. (2.11), has a singularity at the equilibrium condition so its linearisation is not pursued in this work.

The solution to problem (3.4) can then be derived as

$$(\tilde{a}^2-1) + c_3(\tilde{a}-1) = -c_4\tilde{t}, \tag{3.7}$$

where

$$c_3 = \frac{2(1-s_3^{HK}s_2^{IT}/s_1^{IT})}{(s_1^{HK}+s_2^{HK}\overline{c_p}/Le)Pe_0}, \quad Pe_0 = \frac{u_k a_0}{\mathcal{D}_{AB}}, \quad c_4 = \frac{2\bar{\rho}s_4^{HK}}{s_1^{HK}+s_2^{HK}\overline{c_p}/Le}. \tag{3.8a–c}$$

In the large Pe_0 limit, c_3 tends to be zero such that one recovers the classical D^2-law. At small Pe_0, the second linear term becomes dominant so the droplet diameter shrinks linearly with time. The solution for the cases of negligible temperature jump across the Knudsen layer can be found by setting $s_3^{HK}=0$. The lifetime of the droplet τ_{HK} can be found to be $\tau_{HK} = \tau_{D2}(1+c_3)$, where $\tau_{D2} = 1/c_4$ is the droplet lifetime assuming local thermodynamic equilibrium. Therefore, the actual lifetime of an evaporating droplet will be longer than the prediction from the classical D^2-law due to the kinetic-limited regime towards the end.

3.2. *Comparison with experimental data*

To test the validity of the mixed kinetic-diffusion boundary condition, both the numerical results from the full QS problems and the linearised analytical results are compared with the experimental data reported by Jakubczyk *et al.* (2012) and Holyst *et al.* (2013*b*) for the evaporation of triethylene glycol (TEG) and diethylene (DEG) glycol droplets in dry nitrogen and water droplets in humid air. In their experiments, the isolated droplet evaporates very slowly in a nearly isothermal gas domain due to a small gradient in the vapour pressure close to the interface. This enables an accurate time-resolved measurement of the droplet size based on an interferometry technique. Their measurement uncertainty for the droplet size is reported to be up to 10 nm for a single-component droplet (Jakubczyk *et al.* 2012). The physical properties of different fluids and all other parameters used in the model are summarised in table 1. All properties are evaluated from the NIST database (Kroenlein *et al.* 2012), except for $\mathcal{D}_{AB}$ (TEG/DEG in dry nitrogen (Lugg 1968); water in air Massman 1998) and $p^\star$ for TEG and DEG. The saturation pressure $p^\star$ at 298 K for both TEG and DEG is very low and no direct experimental data could be found from

https://doi.org/10.1017/jfm.2023.109 Published online by Cambridge University Press

Substance	M (g mol^{-1})	c_p (kJ kg^{-1} K^{-1})	$p^\star$ (pa)	σ (N m^{-1})	$\mathcal{L}$ (kJ kg^{-1})	ρ_l (kg m^{-3})	$\mathcal{D}_{AB}$ (mm^2 s^{-1})
TEG	150.17	1.398	0.0575	0.04513	527.4	1120	5.9
DEG	106.1	1.386	0.635	0.0432	545.6	1113	7.3
Water	18	4.191	1483.5	0.0738	2470.4	999.35	23.5

Table 1. Physical properties of fluids used in modelling. Both TEG and DEG are evaporated in dry nitrogen at 298 K, 98.7 kPa. Water is evaporated in humid air at 286 K, 99 kPa and 97 relative humidity. The value of λ in dry nitrogen and humid air is 66 and 63 nm, respectively (Holyst *et al.* 2013*b*).

the literature. Therefore, it was taken as the value leading to the best fit of the measured droplet size, in the region where the classical D^2-law is valid, i.e. when the droplet size is sufficiently large so that the kinetic effects are negligibly small ($Pe_k > 30$), and the measurement uncertainty is less than 0.5 %.

The predicted $\tilde{a}^2$ and measured $\tilde{a}^2_{exp}$ and their relative difference, i.e. $(\tilde{a}^2_{exp} - \tilde{a}^2)/\tilde{a}^2_{exp}$, together with the corresponding Pe_k for the evaporation of a water droplet in humid air are shown in figure 2(*a*,*b*). We can clearly see that the classical D^2-law (i.e. assuming local thermodynamic equilibrium and ignore surface tension) becomes increasingly inaccurate as the droplet shrinks (i.e. Pe_k reduces). At large Pe_k, the kinetic process is always much more efficient than the mass diffusion so that the evaporation rate is diffusion limited. However, as the kinetic process becomes less efficient than the mass diffusion for reduced droplet sizes, it becomes the limiting factor and the evaporation rate is decreased. When the surface tension is taken into account, the classical model assuming local thermodynamic equilibrium overestimates the evaporation rate even further, due to the increased saturation pressure at small curvature. Incorporating the mixed kinetic-diffusion boundary conditions with no temperature jump across the Knudsen layer can consistently improve the prediction. However, the extent of improvement is dependent on the magnitude of the temperature jump. When the temperature jump is significant, e.g. evaporation of water in humid air – figure 2(*a*,*b*), the improvement is very limited. In contrast, when the temperature jump is small, e.g. evaporation of TEG/DEG in dry nitrogen shown in figure 2(*c*,*d*), the improvement is very significant. From figure 2, we can also observe that both accommodation coefficients in (1.1) are very close to 1 when the interface is near equilibrium so that negligible differences are introduced by using the semi-empirical HK correlation with unity accommodation coefficients instead of the more rigorous TED-SRT kinetic model. However, the difference will be larger when the evaporation occurs further away from the equilibrium such that there is a larger temperature jump.

From figure 2(*a*), we can also see that incorporating the temperature jump model developed for the evaporation of a droplet in its pure vapour (i.e. (2.14)) yields an unrealistically large temperature jump $\overline{\delta T}$ across the Knudsen layer ($\sim$10 K) and consequentially a significantly slower evaporation rate. A closer look to (2.3) suggests that the large value of $\overline{\delta T}$ stems from the very low equilibrium vapour pressure on the liquid surface, i.e. p_s^{eq} and $\overline{\delta T}$ will diverge as $p_s^{eq} \to 0$, which is not physically acceptable and needs further correction. If the empirical temperature jump model (2.15) is deployed, the QS solution matches the experimental results well in all cases. This good match is a clear indication of the dominant role that the inert gases play in the thermalisation of the vapour molecules emerging from the evaporation. However, the absence of the physical properties of the pure substance (possibly link to the value of A) and the heat flux in this empirical correlation means that it does not account for the energy of the emerging vapour

https://doi.org/10.1017/jfm.2023.109 Published online by Cambridge University Press

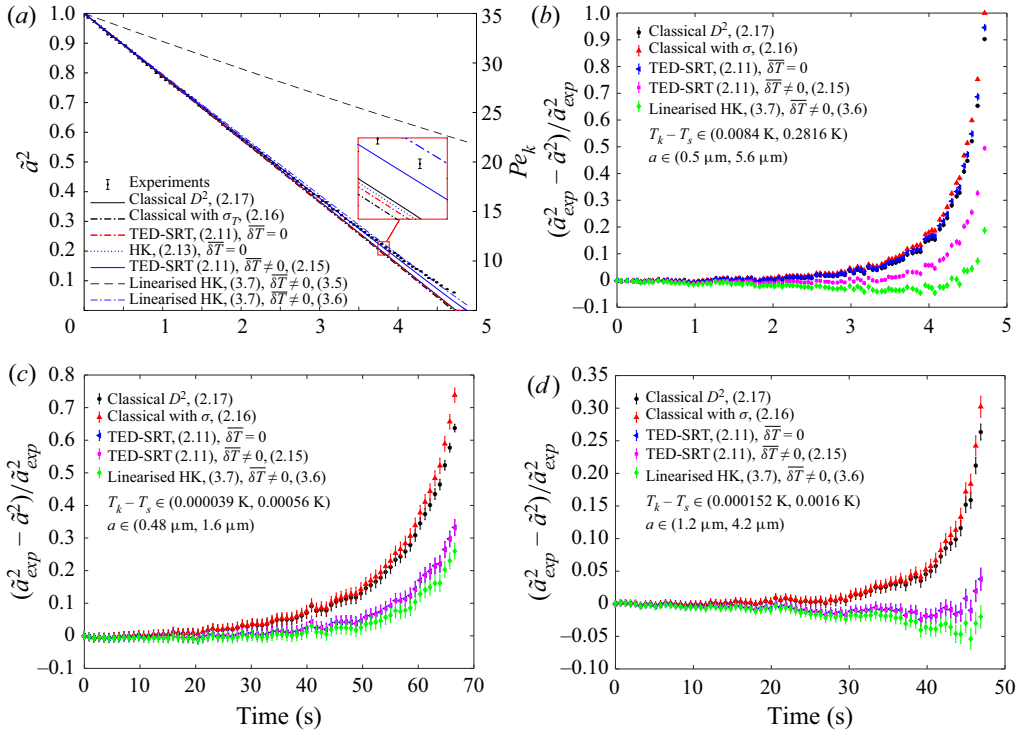

Figure 2. Comparison between the modelled droplet sizes and experimental results. (*a*,*b*) Evaporation of a water drop in humid air (experimental data are from Holyst *et al.* 2013*b*). (*c*) Evaporation of a TEG drop in dry nitrogen (experimental data are from Jakubczyk *et al.* 2012). (*d*) Evaporation of a DEG drop in dry nitrogen (experimental data are from Holyst *et al.* 2013*b*).

molecules properly. The linearised solution, surprisingly, works even better than the full formulation in most cases. This could be an indication that the full formulation needs further revision, possibly through the development of a more rigorous temperature jump model across the Knudsen layer. In summary, among the different models tested, the best option to correct for the error caused by the local thermodynamic equilibrium assumption is to use the mixed kinetic-diffusion boundary condition together with the empirical temperature jump model.

3.3. *Parameter domain study*

To quantify the potential errors induced by the local thermodynamic equilibrium assumption on the prediction of the evaporation rate, we compared the values of B_T calculated at different (Pe_k, Φ_∞), as shown in figure 3(*a*). As expected, the error becomes significant when $Pe_k \leqslant O(10)$ and increases as Pe_k is further reduced. Figure 3(*b*) shows that the errors introduced by neglecting the change in liquid surface chemical potential (due to the presence of inert gas) become significant only when $\bar{\rho} \geqslant O(10^{-1})$, which corresponds to high-pressure or low-temperature conditions. Naturally, as one gets closer to the critical point, the ideal gas law breaks down and a more realistic gas model need to be considered.

https://doi.org/10.1017/jfm.2023.109 Published online by Cambridge University Press

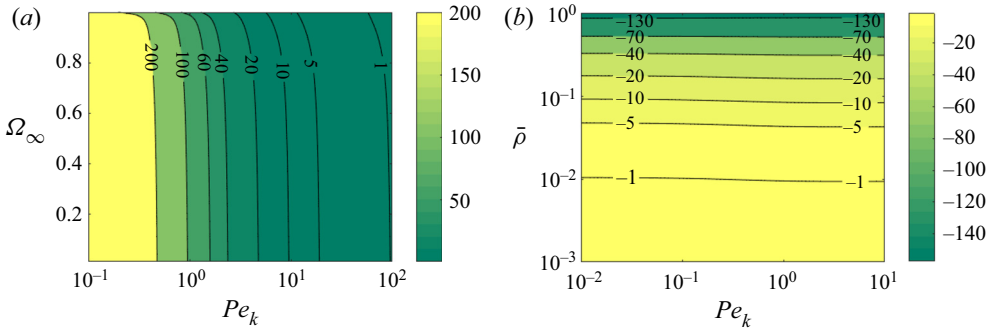

Figure 3. Comparison of B_T values calculated at different conditions. Cases of evaporation of a water drop in humid air ignoring the surface tension effect are considered in this calculation: $Le = 0.8659$, $\overline{c_p} = 0.6031$, $\bar{p} = 0.01$, $Ja = 0.485$, $\gamma = 1.124$, $A = 2.35$, $\lambda = 63$ nm. (*a*) Percentage error coming from the local thermodynamic equilibrium assumption at different $\{Pe_k, \Phi_\infty\}$ when $\bar{\rho} = 1 \times 10^{-3}$; (*b*) percentage error in ignoring the change of liquid phase chemical potential due to the presence of inert gas at different $\{Pe_k, \bar{\rho}\}$ when $\Phi_\infty = 0.98$.

4. Conclusion

In summary, we proposed a more general mixed kinetic-diffusion boundary condition and applied it to solve the QS spherical droplet evaporation problem. The boundary condition formulated here is an extension of the concept of mass conservation across the Knudsen layer introduced by Sultan *et al.* (2005) and accounts for the Stefan flow due to net evaporation, the change of the chemical potential of the interface due to the presence of inert gases and the temperature jump across the Knudsen layer. The mixed boundary conditions are based on either the semi-empirical HK model or the analytical TED-SRT model developed by Persad & Ward (2016). The dimensionless forms of the boundary conditions show that the classical D^2-law, i.e. $a^2 \propto t$, is valid in the large Pe_k limit. In this limit, the kinetics is infinitely fast so that any chemical potential difference across the Knudsen layer is smoothed out and the evaporation rate is limited by the mass diffusion outside the Knudsen layer. As Pe_k reduces, the chemical potential difference across the Knudsen layer starts developing and the local thermodynamic equilibrium assumption breaks down. In the small Pe_k limit, kinetic processes become the limiting factor and the evaporation rate is significantly lower than that predicted by the classical D^2-law. The linearised solution in the slow evaporation limit produces a linear scaling law, i.e. $a \propto t$, in the limit of small Pe_k. Comparison with experimental data available in the literature (Jakubczyk *et al.* 2012; Holyst *et al.* 2013*b*) for the evaporation of TEG, DEG and water droplets suggests that the mixed kinetic-diffusion boundary condition with an empirical temperature jump model (obtained by Holyst *et al.* (2013*b*) through the curve fitting of data obtained from MD simulations) better predicts the evaporation rate compared with the D^2-law, especially in regions where $Pe_k \leqslant O(10)$. It has also noted that the existing temperature jump model based on the evaporation of a droplet in its pure vapour proposed by Struchtrup *et al.* (2017) leads to an unrealistic prediction of the temperature jump across the Knudsen layer, at least when the equilibrium vapour pressure is small, and consequentially is a significant underestimation of the evaporation rate. In comparison, the empirical temperature jump model leads to a much better prediction. However, it does not properly account for the energy feed into the vapour molecules emerging from the evaporation (i.e. no dependency on the heat flux). Therefore, a more rigorous temperature jump model needs to be derived that takes into account both the energy feed into the

https://doi.org/10.1017/jfm.2023.109 Published online by Cambridge University Press

vapour molecules and their thermalisation process due to collisions with the inert gas molecules. At high pressure or low temperature, the increase of the chemical potential at the interface due to the presence of inert gases needs to be accounted for, to better predict the evaporation rate. While the current analysis is limited to the QS evaporation problem, the proposed mixed kinetic-diffusion boundary conditions are applicable to the general problem of droplet evaporation. Accounting for additional effects, such as gas phase transiency, real gas behaviour at high pressure or low temperature and convection both inside and outside droplet, would demand further work.

Acknowledgements. We would like to thank Dr D. Jakubczyk for sharing his experimental data and relevant references.

Funding. This research received no specific grant from any funding agency, commercial or not-for-profit sectors.

Declaration of interests. The authors report no conflict of interest.

Author ORCIDs.
Huayong Zhao https://orcid.org/0000-0002-7651-4329;
François Nadal https://orcid.org/0000-0002-9371-1383.

References

Abramzon, B. & Sirignano, W.A. 1989 Droplet vaporization model for spray combustion calculations. *Intl J. Heat Mass Transfer* **32** (9), 1605–1618.

Burelbach, J.P., Bankoff, S.G. & Davis, S.H. 1988 Nonlinear stability of evaporating/condensing liquid films. *J. Fluid Mech.* **195**, 463–494.

Craster, R.V. & Matar, O.K. 2009 Dynamics and stability of thin liquid films. *Rev. Mod. Phys.* **81** (3), 1131–1198.

Deegan, R.D., Bakajin, O., Dupont, T.F., Huber, G., Nagel, S.R. & Witten, T.A. 1997 Capillary flow as the cause of ring stains from dried liquid drops. *Nature* **389**, 827–829.

Deegan, R.D., Bakajin, O.L., Dupont, T.F., Huber, G., Nagel, S.R. & Witten, T.A. 2000 Contact line deposits in an evaporating drop. *Phys. Rev.* E **62** (1), 756–765.

Finneran, J., Garner, C.P. & Nadal, F. 2021 Deviations from classical droplet evaporation theory. *Proc. R. Soc. Lond.* A **477** (2251), 20210078.

Holyst, R., Litniewski, M., Jakubczyk, D., Kolwas, K., Kolwas, M., Kowalski, K., Migacz, S., Palesa, S. & Zientara, M. 2013*a* Evaporation of freely suspended single droplets: experimental, theoretical and computational simulations. *Rep. Prog. Phys.* **76** (3), 034601.

Holyst, R., Litniewski, M., Jakubczyk, D., Zientara, M. & Woźniak, M. 2013*b* Nanoscale transport of energy and mass flux during evaporation of liquid droplets into inert gas: computer simulations and experiments. *Soft Matt.* **9** (32), 7766–7774.

Jakubczyk, D., Kolwas, M., Derkachov, G., Kolwas, K. & Zientara, M. 2012 Evaporation of micro-droplets: the "radius-square-law" revisited. *Acta Phys. Pol.* A **122** (4), 709–716.

Knudsen, M. 1950 *Kinetic Theory of Gases*. Mehuene.

Kroenlein, K., Muzny, C.D., Kazakov, A.F., Diky, V., Chirico, R.D., Magee, J.W., Abdulagatov, I. & Frenkel, M. 2012 NIST Standard Reference Database 203 Web Thermo Tables (WTT), Professional Edition. National Institute of Standards and Technology. Available at: https://www.nist.gov/mml/acmd/trc/web-thermo-tables-wtt/nist-srd-wtt-203-pro.

Kryukov, A.P., Levashov, V.Y. & Sazhin, S.S. 2004 Evaporation of diesel fuel droplets: kinetic versus hydrodynamic models. *Intl J. Heat Mass Transfer* **47**, 2541–2549.

Lu, Z., Kinefuchi, I., Wilke, K.L., Vaartstra, G. & Wang, E.N. 2019 A unified relationship for evaporation kinetics at low Mach numbers. *Nat. Commun.* **10** (1), 2368–2375.

Lu, Z., Wilke, K.L., Preston, D.J., Kinefuchi, I., Chang-Davidson, E. & Wang, E.N. 2017 An ultrathin nanoporous membrane evaporator. *Nano Lett.* **17** (10), 6217–6220.

Lugg, G.A. 1968 Diffusion coefficients of some organic and other vapors in air. *Anal. Chem.* **40** (7), 1072–1077.

Massman, W.J. 1998 A review of the molecular diffusivities of H_2O, CO_2, CH_4, CO, O_3, SO_2, NH_3, N_2O, NO, and NO_2 in air, O_2 and N_2 near STP. *Atmos. Environ.* **32** (6), 1111–1127.

https://doi.org/10.1017/jfm.2023.109 Published online by Cambridge University Press

MAXWELL, J.C. 1890 *The Scientific Papers of James Clerk Maxwell*. Cambridge University Press.
ORON, A., DAVIS, S.H. & BANKOFF, S.G. 1997 Long-scale evolution of thin liquid films. *Rev. Mod. Phys.* **69** (3), 931–980.
PERSAD, A.H. & WARD, C.A. 2016 Expressions for the evaporation and condensation coefficients in the Hertz–Knudsen relation. *Chem. Rev.* **116** (14), 7727–7767.
POULARD, C., BE, O. & CAZABAT, A.M. 2003 Freely receding evaporating droplets. *Langmuir* **19** (21), 8828–8834.
RANA, A.S., LOCKERBY, D.A. & SPRITTLES, J.E. 2019 Lifetime of a nanodroplet: kinetic effects and regime transitions. *Phys. Rev. Lett.* **123** (15), 154501.
SAZHIN, S.S. 2006 Advanced models of fuel droplet heating and evaporation. *Prog. Energy Combust. Sci.* **32** (2), 162–214.
SIRIGNANO, W.A. 2010 *Fluid Dynamics and Transport of Droplets and Sprays*. Cambridge University Press.
SPALDING, D.B. 1979 *Combustion and Mass Transfer*. Pergamon.
STRUCHTRUP, H., BECKMANN, A., RANA, A.S. & FREZZOTTI, A. 2017 Evaporation boundary conditions for the R13 equations of rarefied gas dynamics. *Phys. Fluids* **29** (9), 092004.
SULTAN, E., BOUDAOUD, A.I. & BEN AMAR, M. 2005 Evaporation of a thin film: diffusion of the vapour and Marangoni instabilities. *J. Fluid Mech.* **543**, 183–202.

https://doi.org/10.1017/jfm.2023.109 Published online by Cambridge University Press